Effect of Polarized Current on the Magnetic State of an Antiferromagnet

Sergei Urazhdin and Nicholas Anthony

Department of Physics, West Virginia University, Morgantown, West Virginia 26506, USA
(Received 14 March 2007; published 26 July 2007)

We provide evidence for the effects of spin polarized current on a nanofabricated antiferromagnet incorporated into a spin-valve structure. The signatures of the current-induced effects include bipolar steps in differential resistance, current-induced changes of exchange bias correlated with these steps, and deviations from the statistics expected for thermally activated switching of spin valves. We explain our observations by a combination of spin torque exerted on the interfacial antiferromagnetic moments and electron-magnon scattering in an antiferromagnet.

PACS numbers: 72.25.Ba, 75.50.Ee, 75.60.Jk, 75.70.Cn

Polarized current flowing through magnetic heterostructures changes the magnetic state of ferromagnets (F) due to the spin transfer (ST) effect [1]. It may find applications in magnetic memory devices, field sensors, and microwave generation. Despite advances in ST devices, their application is still deterred by the large power consumption. The threshold current for the onset of current-induced magnetic precession of a nanomagnet F due to spin transfer is [2]

$$I_c = e2\pi m^2\alpha/(\hbar Vg),\qquad(1)$$

at a small external magnetic field H. Here, e is the electron charge, m and V are the magnetic moment and the volume of the nanomagnet, α is the Gilbert damping parameter, and g is a parameter determined by the transport properties of the structure. I_c is usually close to the current that reverses the magnetization of F.

According to Eq. (1), I_c can be significantly reduced if F has a small magnetic moment m. In nanopatterned magnets, a small m compromises the magnetic stability of devices. However, more complex magnetic systems such as antiferromagnets (AF) can combine vanishing m with a significant magnetic anisotropy and may thus provide both stability and low operating power. Additionally, the possibility to change the magnetic structure of AF by current is attractive for devices utilizing AF for pinning the magnetization of the adjacent F, due to the exchange bias (EB) effect. ST in antiferromagnets has been predicted [3], but experimental studies have been inconclusive [4–6]. Such studies may provide information about the role of electron-magnon scattering in ST phenomena, the nature of enhanced magnetic damping in F/AF bilayers [7], and the properties of the interfacial magnetic moments central to EB.

We report on the effect of polarized current on nanoscale AF layer incorporated in a vertical magnetoresistive (MR) structure $F_1/N/F_2/AF$, with the top F_2/AF bilayer patterned into an 120×60 nm nanopillar. These samples are labeled EB nanopillars. Several important behaviors of our samples can be attributed to the effect of current on AF. First, EB can be changed by applying a pulse of current.

The changes are nonmonotonic and asymmetric with respect to the directions of current and applied field, which eliminates Joule heating as their origin. Second, the changes of the current-induced EB are correlated with the onset of magnetic dynamics. Finally, current-induced magnetization reversal is inconsistent with the standard thermal activation model, indicating a complex current-induced magnetic state of AF.

We tested 8 samples with the structure $Py(30)Cu(10)Py(5)Fe_{50}Mn_{50}(t)Cu(1)Au(10)$, where $Py =$ Permalloy $= Ni_{80}Fe_{20}$, and $1.5 \leq t \leq 4$. All thicknesses are in nanometers. The multilayers were deposited by dc magnetron sputtering at room temperature (RT) in 5 mTorr of purified Ar. Residual impurity pressure during deposition was less than 2×10^{-8} Torr, as verified with a gas analyzer. The samples were fabricated via multistep e-beam lithography procedure described elsewhere [8]. Atomic force microscopy of similarly deposited films indicated roughness of interfaces not exceeding 0.7 nm. The magnetic configuration of nanopillars was determined via four-probe MR measurements between RT and 4.5 K. Current $I > 0$ flowed from the extended to the patterned Py layer, and H was along the nanopillar easy axis.
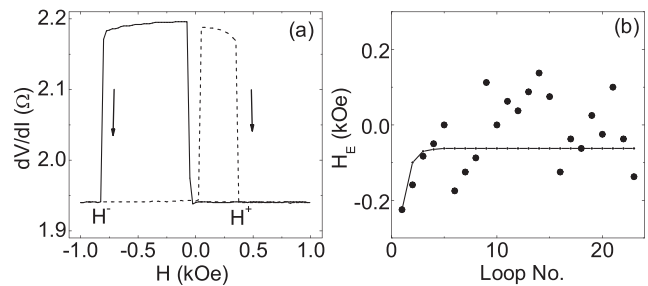

FIG. 1. (a) Hysteresis loop of EB nanopillar acquired at 4.5 K immediately after cooldown at $H = 3$ kOe from 350 K. Reversal fields H^+ and H^- of Py(5) are labeled. (b) Exchange bias H_E vs the hysteresis loop number in EB nanopillar (symbols) and a 5×5 mm sample with magnetic multilayer structure identical to the EB nanopillar (curve).

In contrast to thick FeMn, samples with FeMn (1.5) exhibited only two stable magnetic configurations of the Py(5) nanopillar: parallel (P) and antiparallel (AP) with respect to the extended Py(30). These samples exhibited all the important features of EB associated with FeMn. Therefore, we focus below on the results for one of the two studied EB samples with $t = 1.5$. The data for the EB sample shown in Fig. 1(a) were acquired immediately after cooldown at $H = 3$ kOe from 350 K. Field-induced reversals occurred in a single step at all temperatures T between 4.5 K and RT. Upward jumps of dV/dI in Fig. 1(a) at small $H = \pm 30$ Oe are caused by the reversals of the extended Py(30) layer from the P to the AP state. The asymmetric downward jumps at large $H^+ > 0$ and $H^- < 0$ [labeled in Fig. 1(a)] are caused by the reversal of the Py(5) layer. The asymmetry is due to FeMn and can be characterized by the effective EB field $H_E = (H^+ + H^-)/2 = -225$ Oe. The coercivity is $H_C = (H^+ - H^-)/2 = 588$ Oe.

Very thin FeMn layers usually become magnetically unstable due to the reduced anisotropy energy [9]. Indeed, repeated cycling of H yielded fluctuating values of H_E [symbols in Fig. 1(b)]. This behavior was attributed to reorientation of FeMn among a few metastable states. When similar measurements are performed in an extended film, H_E should quickly decay from the initial value determined by the field cooling, due to the averaging of magnetic fluctuations over a large number of AF grains. This behavior was verified in a 5×5 mm^2 heterostructure Py(5)Cu(10)Py(5)FeMn(1.5)Cu(1)Au(3) magnetically identical to the EB nanopillars [curve in Fig. 1(b)].

The effect of current on the magnetic structure of AF can be determined by applying a pulse of current I_0 at field H_0 and subsequently measuring the hysteresis at a small I not affecting the magnetic state of the nanopillar. The results of such measurements are shown in Fig. 2 for $H_0 = -3$ kOe (a) and $H_0 = 3$ kOe (b). These values of H_0 suppressed current-induced reversal of the Py(5) nanopillar. The data exhibit a sharp increase of H_E up to negative $I_0 = -7.5$ mA, and a positive $I_0 = 5$ mA in Fig. 2(a), for $H_0 =$

-3 kOe. The data in Fig. 2(b) for $H_0 = 3$ kOe are scattered and do not exhibit a clear dependence on I_0. If these changes of H_E were caused by Joule heating of FeMn, the data in Figs. 2(a) and 2(b) would mirror each other, at least for large I_0. Additionally, the effect of heating would increase with I_0, so a monotonic dependence would be expected. Therefore, the effect of current on the magnetic state of FeMn cannot be explained by heating.

Additional evidence for the effects of current on FeMn distinct from Joule heating was provided by the measurements of current-induced behaviors. At small H, Py(5) reversed into the P state at a current I^- and into the AP state at a current I^+, consistent with the ST mechanism [top curve in Fig. 3(c)]. However, the dependencies of I^- and I^+ on T reflected a strong influence of FeMn on the current-induced reversals. Figure 3(a) shows that I^- and I^+ in the standard sample did not significantly depend on T (open symbols), but they increased linearly with decreasing T in the EB nanopillars [10]. This result is consistent with the previously seen enhancement of magnetic damping due to AF [5,7].

Current-induced behaviors of the EB samples were different from the standard ones at large H, as shown in Figs. 3(b) and 3(c). The standard sample exhibited two previously established features [8]. First, switching became reversible and exhibited telegraph noise, resulting in a peak in dV/dI at $I > I_c^+$ [dotted curve in Fig. 3(b)]. The peak rapidly shifted to higher I at larger H. The second feature was a weak increase of dV/dI at $I > I_c^+ \approx I^+$. This feature is associated with the current-induced precession of the Py(5) magnetization [11].

The EB nanopillars did not exhibit a reversible switching peak at any H. The $H = 1$–3 kOe data in Fig. 3(c) show a step at I_c^+ and a linear increase at $I > I_c^+$. Because the position of the step does not significantly depend on H,
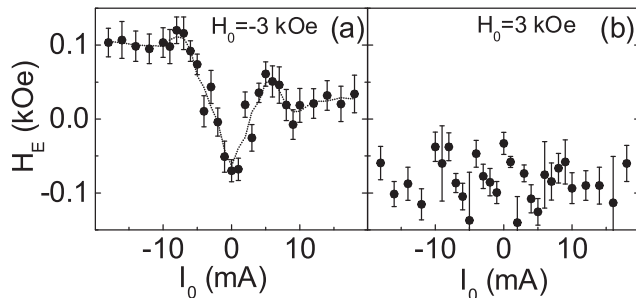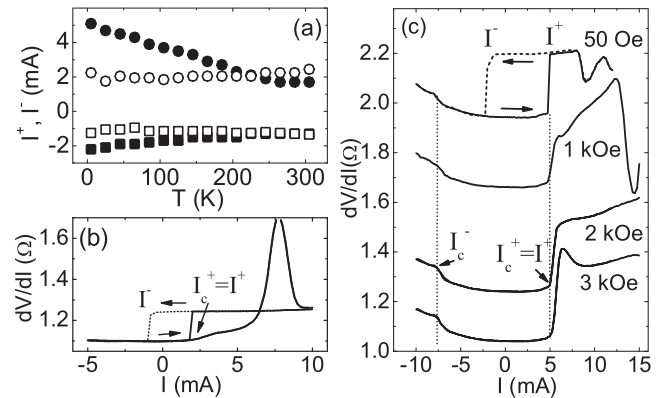

FIG. 2. H_E of EB sample measured at $I = 0.3$ mA after a 100 ms pulse of current I_0 applied at $H_0 = -3$ kOe (a) and $H_0 = 3$ kOe (b). Each point is an average of 10 measurements, whose statistics are represented by error bars. H_0 and/or I_0 were reversed after each group of measurements. The dashed curve in (a) is a guide to the eye.

FIG. 3. (a) Switching currents from P to AP state (circles) and from P to AP state (squares) vs T for EB nanopillar (solid symbols) and standard sample (open symbols), at $H = 50$ Oe. (b) dV/dI vs I at 4.5 K for standard sample, with $H = 50$ Oe (dashed and solid curves), and 363 Oe (dotted curve). (c) Same as (b), but for the EB sample at the labeled values of H. Curves for $H > 50$ Oe are offset for clarity.

it can be attributed to the current-induced precession of Py(5), as confirmed by the time-resolved measurements described below. The step at I_c^+ is correlated with the sharp increase of H_E in Fig. 2(a). Similarly, a smaller step in dV/dI at $I = -7.5$ mA, labeled I_c^- in Fig. 3(c), is also correlated and increase of H_E in Fig. 2(a) at $I < 0$. Both steps are attributed to the current-induced magnetic dynamics, which must therefore play an important role in current-induced EB. To confirm that these steps are associated with the FeMn layer, T was increased to RT. Both steps disappeared, and the reversible switching peak was observed.

To identify the origin of the high-field current-induced behaviors in Fig. 3(c), we performed time-resolved measurements of resistance R. Figure 4(a) shows an example of a time trace acquired at $I = 9$ mA and $H = 900$ Oe. The data show telegraph noise switching between P and AP states, qualitatively similar to the standard sample. However, there are significant quantitative differences. First, the EB nanopillar occasionally spent a significant continuous period of time in the AP state, which was not observed in the standard samples. Second, the average dwell times in the P state (τ_P) and the AP state (τ_{AP}) exhibited a nonmonotonic dependence on I, as illustrated in Fig. 4(b) [12]. In contrast, the standard sample exhibited a monotonic increase of τ_{AP} and a decrease of τ_P with increasing I. The data for the standard sample were consistent with the Néel-Brown model of thermal magnetic activation [13].

The dependencies of average dwell times on I account for the approximately linear increase of dV/dI at $I > I_c^+$ in the EB samples. The origin of these dependencies can be better understood by plotting the distributions of dwell times in the P state (t_P) and the AP state (t_{AP}) [Figs. 4(c) and 4(d)]. t_P closely followed an exponential distribution with a decay time $\tau_0 = 1.1$ ms at $I = 9$ mA and $H = 900$ Oe. Similar distributions were obtained for both t_P and t_{AP} in the standard samples, consistently with the thermal activation model [13]. However, the distribution of t_{AP} for the EB nanopillar was clearly not exponential due to occasionally long dwell times in the AP state. Of the total 10 sec time interval of data analyzed in Fig. 4(d), the system spent one continuous 1.8 s long interval and three 200 ms long intervals in the AP state. The remaining dwell times were predominantly less than 1 ms, as shown in the inset. As I was increased, the intervals of long t_{AP} gradually disappeared, resulting in decreasing τ_{AP} in Fig. 4(b). Simple enhancement of magnetic damping and/or the anisotropy induced by FeMn cannot account for the deviations from the standard exponential distributions. Therefore, this behavior is the strongest evidence in our data for the effect of $I > 0$ on the magnetic state of FeMn, which results in occasional enhancement of Py(5) stability in the AP state.

Before discussing the mechanisms underlying the observed effects of current on the AF/F bilayer, we summarize the current-induced behaviors distinguishing the EB samples from the standard ones: (i) The switching currents depend linearly on T, (ii) the effect of current on H_E is asymmetric with respect to the directions of H and I, (iii) the sharp increases of H_E are correlated with the steps in dV/dI, and (iv) reversible switching exhibits occasionally long dwell times in the AP state.

We analyze our data using a model accounting for the contributions of both the spin current and the spin accumulation to ST at magnetic interfaces [2]. The parameter g in Eq. (1) characterizing ST at the interface N/F_2 is expressed through the known material parameters

$$g = (j_{F2} + v_{F2}m_{F2}/4)e/j, \qquad (2)$$

where j is the current density, $v_{F2} \approx 0.3 \times 10^6$ m/s is the average Fermi velocity in F_2, j_{F2} and m_{F2} are the spin current density and spin accumulation density, respectively, just inside F_2 at the N/F_2 interface. Spin flipping in the Cu spacer is neglected in Eq. (2). The spin accumulation and spin current density were calculated self-consistently throughout the multilayer using the Valet-Fert model [14]. Material parameters known from MR measurements and electron photoemission were used [15,16]. Spin diffusion length of 0.5 nm was used for FeMn. Equation (2) yielded $g = 0.89$ for the P state and $g = -1.88$ for the AP state. Inserting those values into Eq. (1), we obtained good agreement with the switching currents at 4.5 K by assuming $\alpha = 0.12$. This value is in general agreement with $\alpha = 0.03$ for the standard samples [5] and the enhancement of damping due to FeMn, as determined from the temperature dependence of switching currents [Fig. 3(a)].
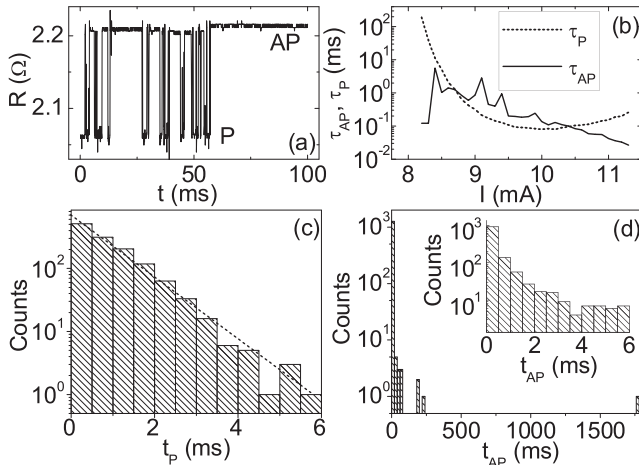

FIG. 4.   (a) R vs t for EB nanopillar at $I = 9$ mA, $H = 900$ Oe. (b) Average dwell times in the P state τ_P (dashed curve) and the AP state τ_{AP} (solid curve) vs I, at $H = 900$ Oe. (c) Distribution of dwell times in the P state at $I = 9$ mA and $H = 900$ Oe. Dashed line is exponential fit with characteristic time $\tau_0 = 1.1$ ms. (d) Same as (c), for the AP state. Inset shows the distribution for the shorter time scale.

A calculation for the Py/FeMn interface yielded a positive $g = 1.2$ for the P state, implying that FeMn moments that are noncollinear to Py experience a spin torque favoring their P configuration with Py(5) for $I < 0$ and AP configuration for $I > 0$. Exchange interaction tends to align the interfacial Mn moments in FeMn antiparallel to the adjacent F and Fe moments parallel to it [17]. The latter have a larger magnetic anisotropy and likely dominate the EB. The following picture of ST at the Py/FeMn interface then emerges. The positive value of g at the Py/FeMn interface implies that ST acting on the interfacial Fe moments enhances EB for $I_0 < 0$ and suppresses it for $I_0 > 0$, explaining the asymmetry with respect to the current direction in Fig. 2(a), for $H_0 = -3$ kOe. A step in dV/dI at I_c^- is likely caused by the current-induced precession of the stable Fe moments that remain antiparallel to the Py magnetization, consequently inducing dynamical Py response resulting in MR.

The asymmetric current-induced behaviors in Fig. 2(a) are superimposed on the symmetric enhancement of EB, independent of the current direction. We propose two possible mechanisms. First, electron-magnon scattering at the Py/FeMn interface may activate transitions of the FeMn magnetic moments into the orientation dictated by the magnetization of the adjacent Py. A second, probably weaker, effect may be due to a torque on the Fe moments exerted by the Oersted field of I, assisting their rotation into the direction parallel to the Py moments. The sharp increases of EB at I_c^+ and I_c^- support the activation picture, since magnetic dynamics excited in FeMn either directly by ST, or indirectly through interaction with precessing Py, should assist in activating the transition of the interfacial AF magnetic moments into the configuration defined by the in-field cooling.

To interpret the lack of significant current dependence of EB on I_0 for the $H_0 = 3$ kOe data, we note that the average H_E in Fig. 2(b) is independent of I_0 and is similar but opposite in sign to the largest values obtained for $H_0 = -3$ kOe. Therefore, it is possible that at $H_0 = 3$ kOe, the AF simply reverts to the configuration defined by the in-field cooling. We note a smaller scatter of the $H_0 = -3$ kOe data compared to the $H_0 = 3$ kOe data in Fig. 2, likely caused by the simpler energy profile of the current-induced metastable state of AF. However, this tentative interpretation warrants additional theoretical modeling.

We also propose an interpretation for the nonexponential distribution of t_{AP} in Fig. 4(d). A simple enhancement of the AP state stability due to EB cannot be responsible because then t_P would also exhibit a similar effect. Therefore, the occasionally long t_{AP} are likely caused by the current-induced enhancement of magnetic stability, efficient only in the AP state at $I > 0$, but not in the P state. Since $I > 0$ suppresses the fluctuations of the magnetic layer in the AP state, due to the ST in the standard samples [13], a similar combined effect of current on both

F and AF layers likely takes place in the EB samples. It is efficient only for some of the magnetic configurations that FeMn acquires due to the fluctuations, specifically those minimizing the current-induced precession of Fe moments, resulting only in occasional enhancement of t_{AP}.

In summary, we demonstrated that spin polarized electron current affects the magnetic state of an antiferromagnet. The effect is distinct from Joule heating and is explained by a combination of a current-induced excitation of antiferromagnetic moments by spin transfer and electron-magnon scattering at the magnetic interface. This mechanism may be useful for establishing exchange bias in nanoscale magnetoelectronic devices.

[1] J. A. Katine, F. J. Albert, R. A. Buhrman, E. B. Myers, and D. C. Ralph, Phys. Rev. Lett. **84**, 3149 (2000).

[2] A. Fert, V. Cros, J.-M. George, J. Grollier, H. Jaffres, A. Hamzic, A. Vaures, G. Faini, J. Ben Youssef, and H. Le Gall, J. Magn. Magn. Mater. **272–276**, 1706 (2004).

[3] A. S. Nunez, R. A. Duine, P. Haney, and A. H. MacDonald, Phys. Rev. B **73**, 214426 (2006).

[4] J. Hayakawa, H. Takahishi, K. Ito, M. Fujimori, S. Heike, T. Hashizume, M. Ichimura, S. Ikeda, and H. Ohno, J. Appl. Phys. **97**, 114321 (2005).

[5] N. C. Emley, I. N. Krivorotov, O. Ozatay, A. G. F. Garcia, J. C. Sankey, D. C. Ralph, and R. A. Buhrman, Phys. Rev. Lett. **96**, 247204 (2006).

[6] Z. Wei, A. Sharma, A. S. Nunez, P. M. Haney, R. A. Duine, J. Bass, A. H. MacDonald, and M. Tsoi, Phys. Rev. Lett. **98**, 116603 (2007).

[7] J. Dubowik, F. Stobiecki, I. Goscianska, Y. P. Lee, A. Paetzold, and K. Roll, J. Korean Phys. Soc. **45**, 42 (2004).

[8] S. Urazhdin, N. O. Birge, W. P. Pratt, Jr., and J. Bass, Phys. Rev. Lett. **91**, 146803 (2003).

[9] J. Nogues and I. K. Schuller, J. Magn. Magn. Mater. **192**, 203 (1999).

[10] The slight increase of I^-, I^- at $T > 250$ K is caused by the shunting currents through the Si substrate.

[11] S. I. Kiselev, J. C. Sankey, I. N. Krivorotov, N. C. Emley, R. J. Schoelkopf, R. A. Buhrman, and D. C. Ralph, Nature (London) **425**, 380 (2003).

[12] Fluctuations of τ_{AP} in Fig. 4(b) are caused by occasionally large t_{AP} discussed in the text.

[13] Z. Li and S. Zhang, Phys. Rev. B **69**, 134416 (2004).

[14] T. Valet and A. Fert, Phys. Rev. B **48**, 7099 (1993).

[15] K. N. Altmann, N. Gilman, J. Hayoz, R. F. Willis, and F. J. Himpsel, Phys. Rev. Lett. **87**, 137201 (2001).

[16] J. Bass and W. P. Pratt, Jr., J. Magn. Magn. Mater. **200**, 274 (1999).

[17] W. J. Antel, Jr., F. Perjeru, and G. R. Harp, Phys. Rev. Lett. **83**, 1439 (1999); F. Offi, W. Kuch, L. I. Chelaru, K. Fukumoto, M. Kotsugu, and J. Kirschner, Phys. Rev. B **67**, 094419 (2003).